A Toolkit for Tailoring Ice-Templated Scaffold Structure

K. M. Pawelec, A. Husmann, S. M. Best, R. E. Cameron

October 16, 2013

In this paper we prove for the first time the key link between scaffold architecture and latent heat evolution during the production of porous biomedical collagen structures using freeze drying. Collagen scaffolds are used widely in the biomedical industry for the repair and reconstruction of skeletal tissues and organs. Freeze drying of collagen slurries is an industry standard, and until now, literature has sought to characterize the influence of set processing parameters including the freezing protocol and weight percentage of collagen. However, we are able to demonstrate, by monitoring the local thermal events within the slurry during solidification, that nucleation, growth and annealing processes can be controlled, and therefore we are able to control the resulting scaffold architecture. Based on our correlation of thermal profile measurements with scaffold architecture we hypothesize that there is a universal link between the fundamental freezing of ice and the structure of scaffolds which suggests that this concept is not only applicable for collagen, but also for ceramics and pharmaceuticals. We present a toolkit of strategies for tailoring the ice templated scaffold structure.

1 Introduction

Collagen scaffold architecture is vital to controlling mechanical properties and cellular interactions within tissue engineering scaffolds [1, 2, 3, 4]. With ice templating techniques, scaffold pores are formed as ice crystals nucleate and grow, concentrating solids, consisting of collagen and acetic acid, between crystals. Once the ice is subsequently removed during lyophilization, an interconnected scaffold mirroring the ice crystal structure remains. Thus, scaffold structure is heavily dependent on the ice crystallization within a slurry.

The crystallization of ice is a complex process, involving nucleation and crystal growth, both of which are heavily influenced by thermal history and properties of the liquid. Nucleation is often considered the defining moment of ice structure determination, and is pivotal to determining whether scaffolds are isotropic or anisotropic [5, 6, 7]. Accordingly, literature has focused on controlling when and where nucleation will occur to alter the final structure of the

scaffold. Large set cooling rates, often produced by liquid nitrogen quenching, can alter the pore anisotropy by creating large temperature gradients within the volume of the slurry [8]. On the other hand, moderate set cooling rates have no power to alter the isotropy of a scaffold structure, although shifts between 0.6 - 0.9 °Cmin^{-1} have been shown to change the pore size between 120 and 90 μm, respectively [9].

The final pore structure, whether anisotropic or isotropic, is determined, not only by the nucleation of ice, but the subsequent growth of ice crystals. Ice crystal growth is strongly influenced by the system in which the freezing occurs and the temperature at which solidification takes place [10]. The growth of ice has been linked to the freezing protocol used to solidify the structure. It has been found that as the set freezing temperature decreases the pore size decreases as well [11]. Also, the addition of a thermal hold to the freezing protocol has been shown to coarsen scaffold architecture and increase the pore size, as the structure anneals and larger ice crystals grow at the expense of smaller ones [12, 13, 14]. While the term annealing can commonly refer to both crystal growth effects or thermal processing steps, in the current study "annealing" refers to the rearrangement of crystal structure and a "thermal hold" refers to a step within the set freezing protocol which encourages crystal structures to rearrange. The effects of annealing become more pronounced as the length and temperature of the thermal hold increase [6, 14]. As the freezing protocol influences crystal growth, changes to the freeing protocol have produced large ranges of pore sizes, ranging from 80 - 320 μm, of interest for tailoring scaffolds for diverse cell types.

Although anisotropic scaffolds have the ability to mimic complex tissues such as tendon and cardiac muscle, the majority of tissue engineering scaffolds are isotropic [2, 15]. As regenerative medicine begins to make strides, tissue engineering scaffolds are needed which are large enough to span critical sized defects, often larger than 10 mm in every direction. Thus, literature focusing on thin scaffolds, 3 mm thickness or less, must be adapted to create scaffolds with dimensions greater than 10 mm.

While the biological activity of a tissue engineering scaffold depends on scaffold architecture, little is known about how scaffold pore size is related to the physics underlying the ice templating process. Previous literature has focused on how pore size is influenced by changing set processing variables, such as set final freezing temperature and thermal holds steps, without looking at the physics underlying ice crystallization. No clear link between pore structure and thermal parameters during the freezing process has been established.

Within the current study, we have defined key thermal parameters from the local thermal profiles and freezing characteristics of the slurry. By varying the set freezing protocol, a large range of pore structures was created and, for the first time, it is shown that the pore size can be predicted by thermal parameters. The principal is demonstrated with isotropic scaffolds larger than 10 mm in all directions, regardless of the processing: set freezing protocol, slurry composition, filling height, or mold design. A universal link should prove a powerful tool to predict scaffold structure from the freezing behavior. With the previous work elucidating the

mechanisms of anisotropic growth, it is believed that these form the basics to understanding and ultimately mastering the structures formed via ice-templating technology.

2 Methods

2.1 Collagen Scaffold Production

Suspensions of 1 wt% bovine Achilles tendon, type I collagen (Sigma Aldrich) were prepared by hydrating in 0.05M acetic acid overnight, then adjusting the pH to 2 before homogenization at 13,500 rpm for 30 minutes in an ice water bath (VDI 25, VWR International Ltd, UK). Slurries were centrifuged (Hermle Z300) at 2500 rpm for 5 minutes and poured into a perspex mold with a standard cylindrical shape: inside diameter of 20 mm and a height of 30 mm, Figure 1. The slurry height was 15 mm, corresponding to 5.7 ml collagen.

Freezing parameters were varied in several ways; it is important to note that variables which were controlled during the freezing cycle, were denoted as "set" to differentiate them from local freezing events. The set final freezing temperature, or the temperature which the freeze drier shelf reached during the freezing cycle, varied between: -20 °C, -30 °C, and -40 °C . While the freezing temperature changed, the set cooling rate remained constant at 0.9 °Cmin^{-1}. A protocol with a thermal hold was also tested, where slurry was cooled to -30 °C, at a set cooling rate of 0.9 °C$min^{-1}$and held for 10 minutes to ensure primary nucleation occurred. The set freezing temperature was then raised to -14 °C and held for 3 hours. After freezing was completed, slurries were lyophilized using a Virtis freeze drier (SP Industries, USA) at 0 °C for 20 hours under a vacuum of less than 100 mTorr.

2.2 Thermal Characterization

Thermocouples, part of the Virtis freeze drier (SP Industries, USA), recorded the thermal profiles of the slurry at the base and top, taking measurements every 10 seconds. The cooling rate of the shelf-ramping lyophilizer was termed the set cooling rate and the set final freezing temperature refers to the set temperature of the shelf during the freezing cycle which was varied during the study, Figure 1.

From the thermal profiles, several parameters were quantified: nucleation temperature, cooling rate of the slurry, freezing time, and time at equilibrium. Nucleation temperature was defined as the temperature, below the equilibrium freezing temperature (0°C), which the slurry reached before latent heat release caused the temperature to jump back to equilibrium. Freezing was initiated when the nucleation temperature was reached. The end of freezing was defined as the extrapolated point at which the initial slope of the thermal line changed. Freezing time was measured between these two points. Time at equilibrium was the time at which the slurry remained above the equilibrium cut-off temperature, set at -1.5 °C, and further discussed in the

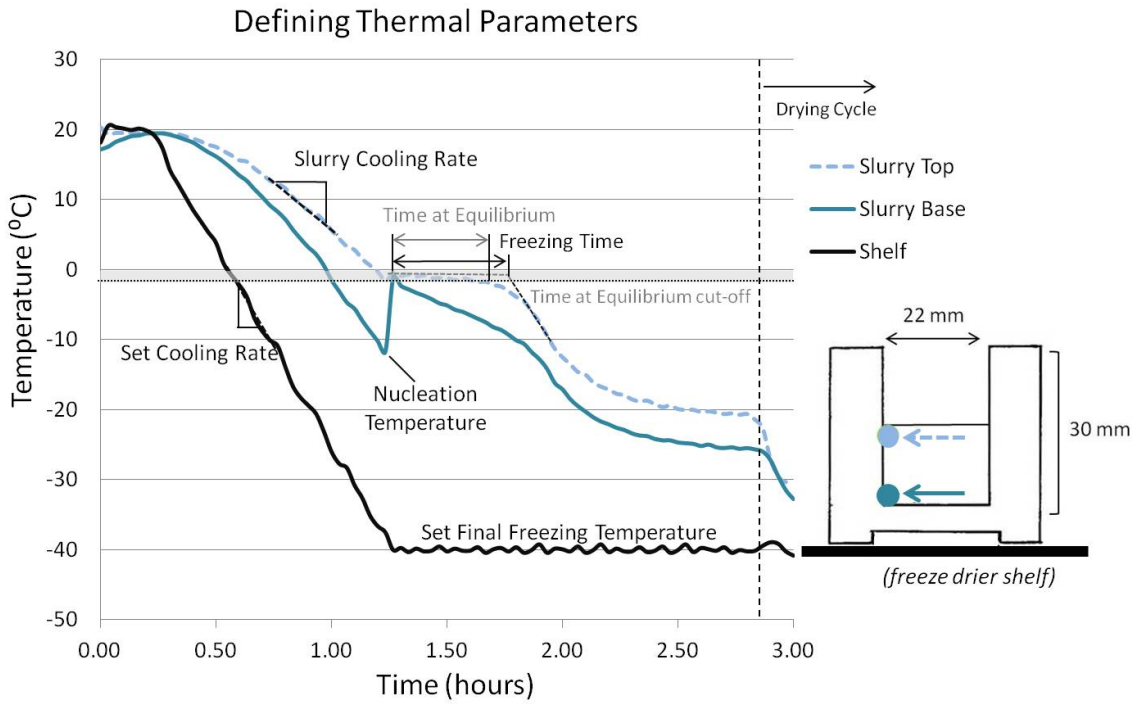

Figure 1: Thermal profiles were used to quantify several thermal parameters: nucleation temperature, cooling rate, freezing time, and time at equilibrium. The set final freezing temperature and set cooling rate were controlled as part of the freezing protocols.

results section. Figure 1 illustrates the parameters measured.

2.3 Scanning Electron Microscopy

Scanning Electron Microscopy (SEM) micrographs were used to visualize the pore structure. All micrographs were taken using a JEOL 820, with a tungsten source, operated at 10 kV.

2.4 Pore Size Analysis

Pore size analysis was done via the line-intercept method on micro-computed tomography images (Skyscan 1072). For each measurement, twelve sections, three lines per slice, from the scaffold were analyzed. All scans were taken at 75x magnification, with a voltage of 25kV, current of 132 μA, and exposure time of 7.5 seconds. Reconstructions were performed with the software program NRecon, part of the Skyscan system.

2.5 Statistics

For each change in the freeze drier protocol, a sample size of 3 was used. A confidence interval of 95% was used throughout and groups were compared via Student's t.

2.6 Differential Scanning Calorimetry

To characterize the melting process, differential scanning calorimetry (DSC, TA Instruments Q2000) was used. In all cases, sample size was about 10 mg. Cooling and warming rates were 2 °Cmin^{-1}. The samples were initially held at 25 °C and cooled down to -25 °C. Nucleation occurred at around -19°C in both samples. It should be noted that the cooling rates were faster than in the freeze dryer and the nucleation temperature was significantly lower than in the molds. The sample size was also much smaller.

3 Results

3.1 Defining Time at Equilibrium

DSC was used to study the melting behavior of the collagen slurry compared to pure water, Figure 2. It was found that the machine could not characterize the melting of pure water, as the release of latent heat occurred too rapidly for the machine to counterbalance. However, it was noted that the onset of melting in pure water was a sharp peak at 1 ºC, Figure 2. With the addition of collagen, the melting peak became broader, and no sharp onset was observed. With no sharp onset visible in DSC, the cutoff for the equilibrium was defined as -1.5 ºC, which is a temperature before the onset of bulk water melting, when large scale molecular movement within the ice-water system is completed.

3.2 Effect of Freezing Protocol on Thermal Parameters

The change in set freezing temperature produced significant changes to the thermal profiles of the slurry at the top and base of the scaffolds, Figure 3, and thus changed the thermal parameters. The *slurry cooling rate* at both the base and the top of the scaffolds increased significantly as the final set freezing temperature decreased from -20 °C to -40 °C, Figure 4. The minimum cooling rate was achieved at a set freezing temperature of -40 °C, -0.46 and -0.65 °Cmin^{-1} at the slurry top and base, respectively.

The *nucleation temperature* was most affected by the change in freezing protocol at the base of the slurry. At the mold base, the nucleation temperature was significantly higher, -8.4 °C, when the set freezing temperature was -20 °C. For all other freezing protocols, including thermal holds, the differences in nucleation temperature at the base were not significant and averaged -11 °C. At the top of the slurry, there were no significant differences in the slurry nucleation temperature.

It was found that as the set freezing temperature increased from -40 °C to -20 °C, the *freezing time* increased significantly from 30 to 90 minutes, Figure 5. While the addition of an annealing step at -14 °C did not change the freezing behavior before primary nucleation, it

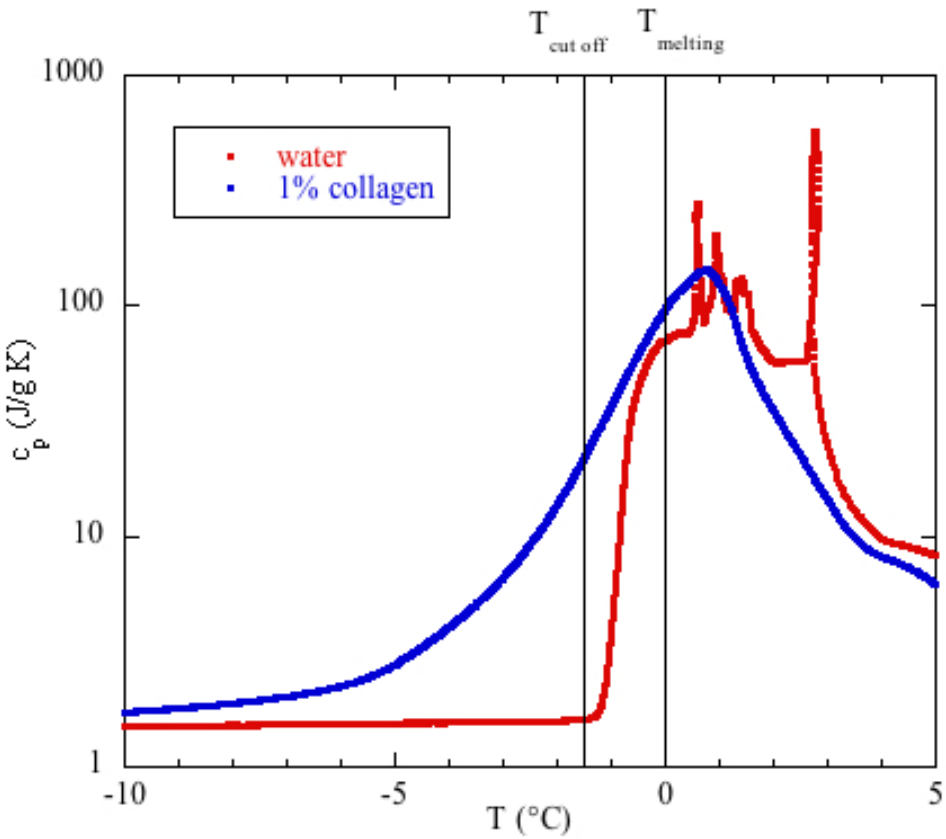

Figure 2: A semi-log plot of the specific heat capacity as a function of temperature. While collagen slurry has no clear onset of melting, water has a sharp transition; the discontinuities in the curve represent the inability of the DSC setup to keep up with the latent heat release. A temperature of -1.5 ºC was chosen as the cut-off for the equilibrium temperature.

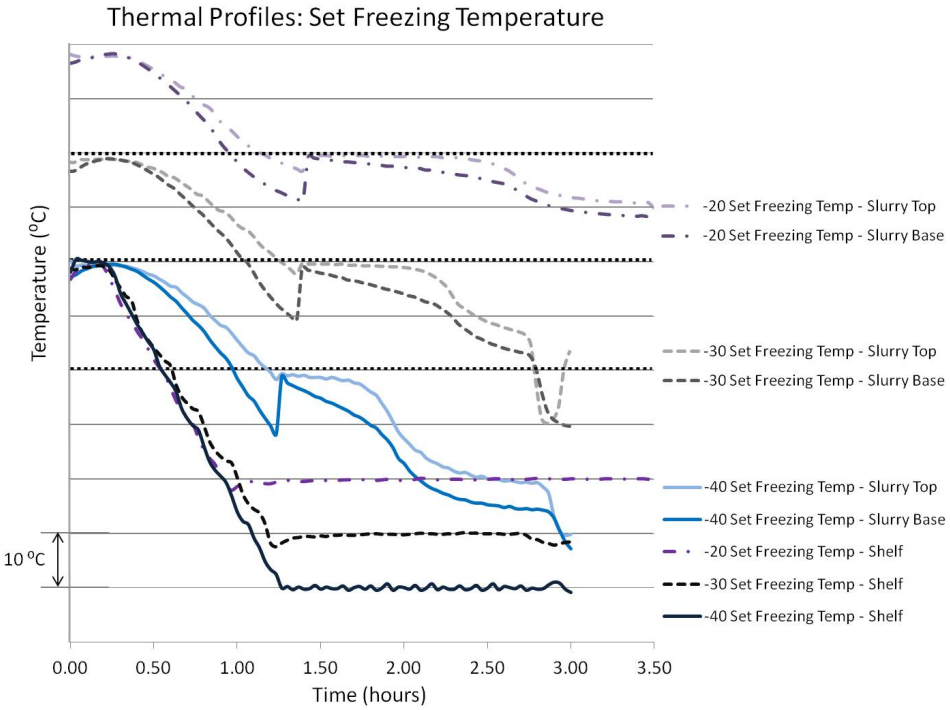

Figure 3: As the set freezing temperature changed from -20 °C to -40 °C, the time until nucleation increased, as did the freezing time. The bold lines mark the equilibrium freezing temperature of each set of thermal profiles.

affected freezing time significantly. With a thermal hold, freezing time was lengthened to 9000 seconds (150 minutes).

At the top of the slurry, the *time at equilibrium* followed the same trend as the freezing time. However, unlike freezing time, the time at equilibrium was dependent on the position within the mold, Figure 5. At the top of the mold, the time at equilibrium increased significantly as the set final freezing temperature increased from -40 °C to -20 °C, reaching a maximum of 9000 seconds (150 minutes) with a thermal hold step. At the base of the mold only the slurry with a set freezing temperature of -20 °C had a significantly higher time at equilibrium, 920 seconds (15 minutes).

3.3 Scaffold Architecture and Freezing Protocol

All of the scaffolds were completely isotropic, with a pore size which was significantly affected by the change in freezing protocol at both the top and base of the scaffolds. At the base of the scaffolds, the pore size ranged from 90 to 115 μm, with the largest pore size reported when the set freezing temperature was -20 °C. At the scaffold top, the largest pore size, 197 μm, occurred in scaffolds which had been through a thermal hold step . The pore size of the scaffolds decreased to 142 μm as the set freezing temperature decreased to -40 °C. In all cases, the pore size at the top of the scaffold was significantly different from the pore size at the base

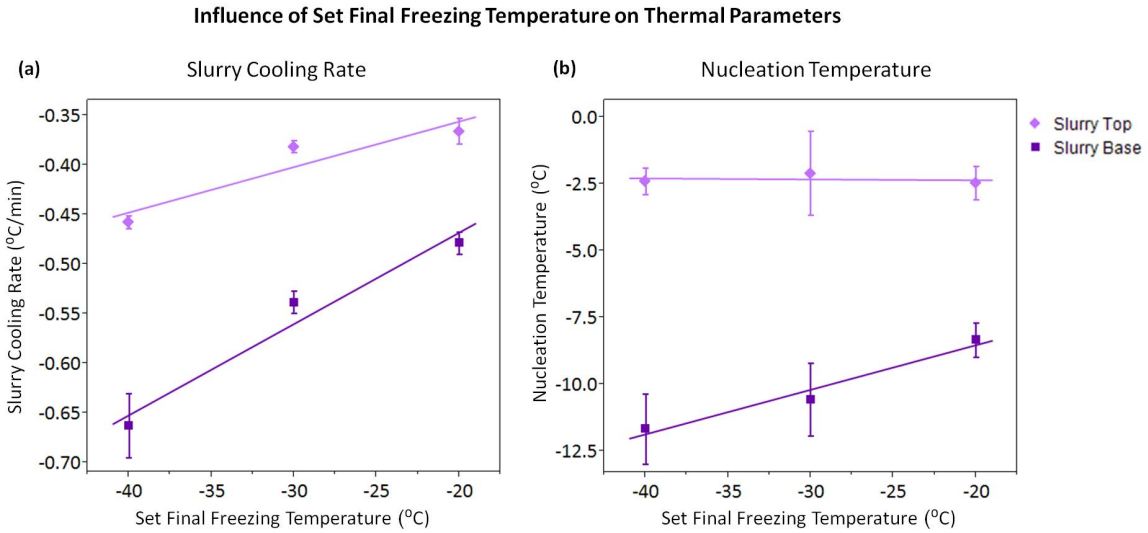

Figure 4: Changes to the set freezing temperature of a collagen slurry resulted in significant changes to thermal parameters: (a) cooling rate, (b) nucleation temperature. The base of the slurry was more affected by the change in freezing protocol than the top of the slurry.

of the mold.

3.4 Relating Scaffold Architecture to Thermal Parameters

As the goal of this study was to link the pore size of isotropic scaffolds to a single thermal parameter, regardless of processing conditions, data was pooled from a previous study to evaluate the fit of the curve [7, 16]. It was found that of all the thermal parameters tested, the time at equilibrium had a very strong relationship to pore size, Figure 7. The curve appeared to be universal, incorporating all of the data points, irrespective of the changes to slurry, filling height or the set freezing protocol. The changes to the freezing protocol, specifically the thermal hold, set the limits of the curve. Curve fitting revealed that pore size was related to time at equilibrium by a power of 4.8.

4 Discussion

4.1 Defining Time at Equilibrium

Tissue engineering is becoming an important tool of regenerative medicine, and as such, the demands on tissue engineering scaffolds continue to increase. Not only must scaffolds be large enough to span larger critical defects of at least 10 mm, but scaffolds must possess a tailored structure to allow cellular infiltration. Understanding the underlying process of ice crystallization, and how it relates to the final scaffold architecture, is key to accomplishing both goals.

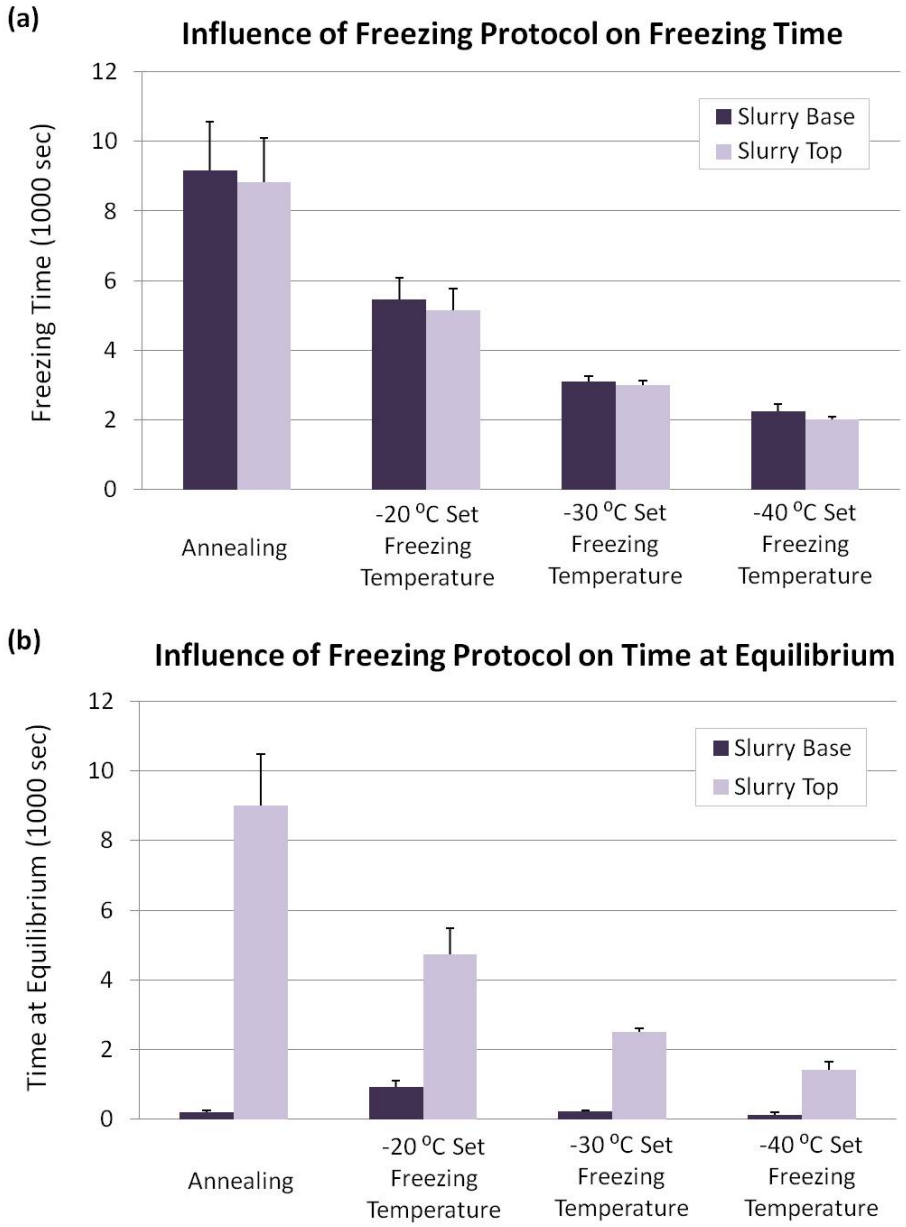

Figure 5: After nucleation, the freezing protocol of the slurry had a significant effect on crystallization, as shown by the (a) freezing time and (b) time at equilibrium. As the set freezing temperature decreased, freezing time and time at equilibrium decreased. A thermal hold lengthened both the freezing time and the time at equilibrium. (1000 seconds is 0.28 hours.)

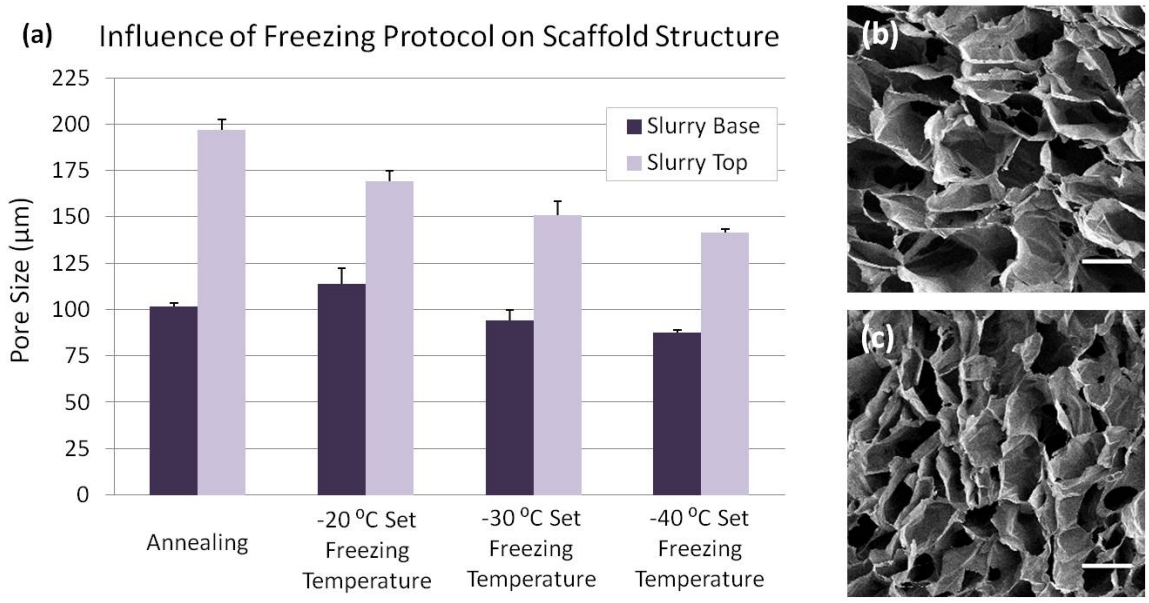

Figure 6: The influence of the set freezing temperature and the thermal hold step on the final pore size of the scaffold at the top and base. (a) Pore size varied significantly at the scaffold top, although the pore size at the base remained relatively unchanged with changes in set freezing protocol. At the scaffold top the (a) maximum pore size occurred in scaffolds with a thermal hold, and the (b) minimum occurred when the set freezing temperature was -40 ºC. Scale bar is 200 µm.

Solidification is commonly described by thermal parameters such as nucleation temperature and freezing time. However, none of these thermal parameters encompass the changes in structure due to crystal growth and annealing, which has been shown to have a significant impact on ice [17]. Molecular movement near equilibrium has been demonstrated to affect not only crystal size, but can also contribute to phenomenon such as phase separation in polymer systems [6, 18, 17]. To capture the effects of annealing on the crystal structure, it was necessary to define a new thermal parameter: time at equilibrium, or the time at which the slurry spends in a temperature range where crystal growth is most actively occurring around the equilibrium freezing temperature. Thus, the time at equilibrium is a measure of how long crystal growth occurred, while the freezing time is a measure of the efficiency of latent heat removal during freezing. It was found, using differential scanning calorimetry (DSC) that, unlike pure water, a gradual increase in molecular activity within the collagen slurry began at -5 ºC with no sharp onset to define melting. As the structure of collagen scaffolds is dependent on ice crystal growth, it was chosen to define the equilibrium cut-off as -1.5 ºC when the majority of molecular activity in ice had ended.

4.2 Effect of Freezing Protocol on Thermal Parameters

In order to create a robust link between thermal parameters and scaffold architecture, the widest range of scaffold structures possible had to be obtained. Set freezing protocols have been shown

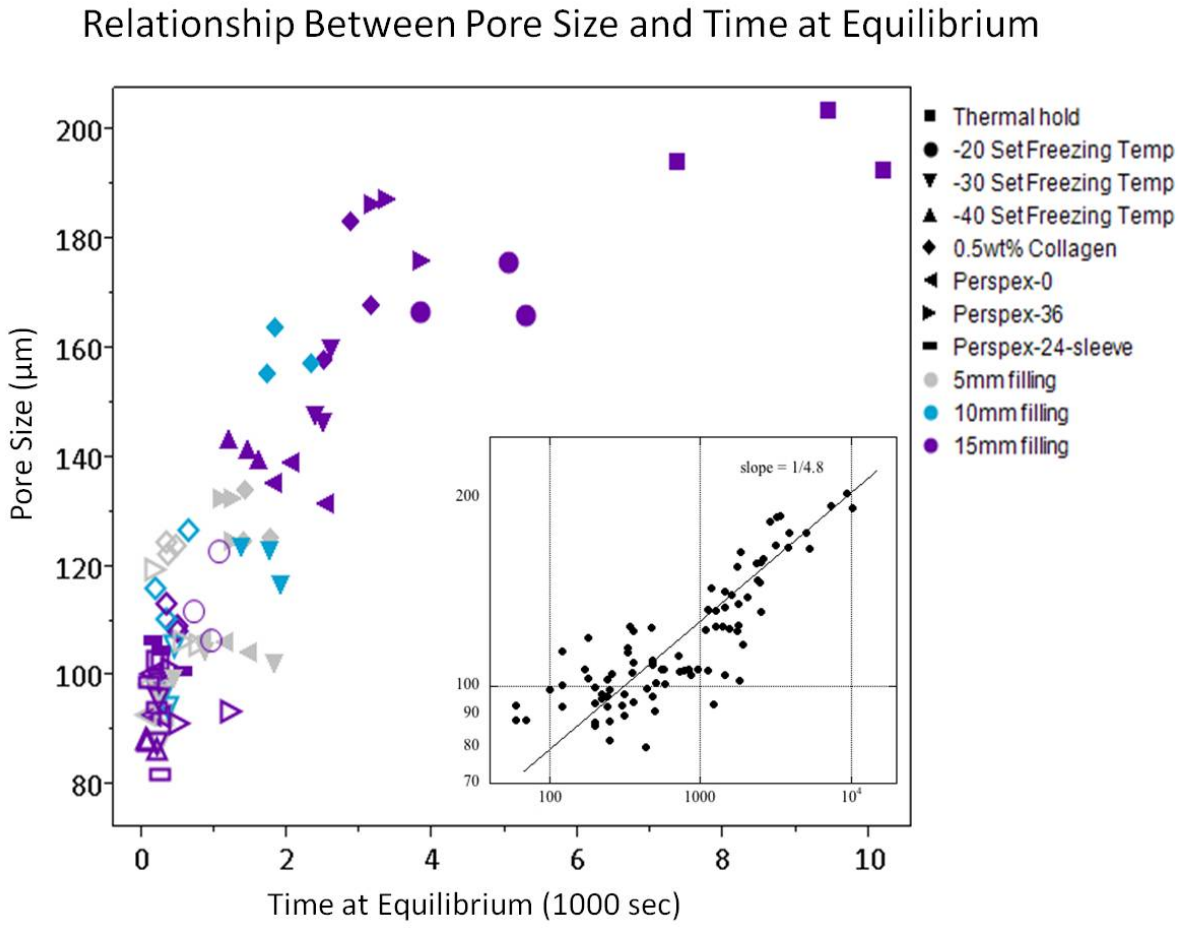

Figure 7: The relationship between time at equilibrium and pore size appeared to be universal regardless of changes to the slurry, the mold design or freezing protocol. Inset: the slope of the curve was $1/n$, where n = 4.8. Closed markers: measurements at the top of slurry, open markers: base of slurry. [7, 16]

in the literature to have a profound effect on pore size [14]. Thus, it was chosen to vary the set final freezing temperature and to add a thermal hold step of a scaffold to expand the range of scaffold pore sizes within this study.

The *slurry cooling rate* decreased significantly at both the top and base of the slurry as the set freezing temperature increased. The trend was especially noticeable at the base of the slurry, the area of the slurry which was most influenced by the heat sink, in this case the freeze drier shelf. Lowering the set freezing temperature led to the creation of larger temperature gradients between the heat sink and the slurry, which in turn induced faster cooling at both the base and top of the slurry.

At the base of the scaffolds, the *nucleation temperature* was significantly different only when the set freezing temperature was -20 ºC. Due to the thermal resistance across the perspex mold, the slurry could not cool below -9 ºC when the set freezing temperature was -20 ºC. As a consequence, the nucleation temperature was significantly higher and only occurred after a large lag time, which is related to the amount of cooling below the equilibrium temperature [19]. In fact, primary nucleation, driven by the base of the scaffold, occurred more rapidly as the set freezing temperature decreased. At the top of the slurry there were no significant differences in nucleation temperatures. The change in the cooling rate at the top of the slurry was effectively canceled out by the reduced lag time before nucleation.

The *freezing time*, which is a measure of ongoing crystallization and the removal of latent heat, was significantly affected by all changes to the freezing protocol. The reduction of freezing time with decreased set freezing temperature was driven by the efficiency of the heat sink, which increases as the set freezing temperature decreases, as has been noted in literature [10]. The addition of a thermal hold reduced the efficiency of the heat sink and led to the longest freezing time recorded.

Like freezing time, the *time at equilibrium* was influenced by the movement of latent heat within the slurry volume. However, the greatest effects were observed at the top of the scaffolds, where latent heat removal is most difficult. Not only did the time at equilibrium increase with set freezing temperature, but with the addition of a thermal hold.

The removal of heat, either sensible heat or latent heat, was the aspect most affected by the change in the freezing protocol. Before primary nucleation, the efficiency of the heat removal was increased with decreasing set freezing temperature. The thermal hold only affected slurry freezing after nucleation, during the growth phase of crystallization. Thus, the two parameters which are correlated to crystal growth, freezing time and the time at equilibrium, were sensitive to both the set freezing temperature and the thermal hold.

4.3 Scaffold Structure: Influence of Freezing Protocol

While all scaffold structures were completely isotropic, the freezing protocol had a significant effect on pore size. At the top of the scaffold, the pore size decreased as the set freezing

temperature decreased, a similar trend to what has been reported previously in 3 mm thick scaffolds [11]. While the nucleation temperature is often cited as predictive measure of pore size, in the present study no significant differences in nucleation temperature were visible at the top of the scaffolds where the change in pore size was the greatest. Instead, it is believed that the efficiency of latent heat removal determined the final pore size, as it has already been noted that set freezing temperatures which are sufficiently high can slow crystallization enough to allow annealing to occur before the end of solidification [20]. Unsurprisingly, as a clear link between annealing and increased crystal size has already been established, the largest pore size, 200 μm, occurred after the addition of an intentional thermal hold [6].

At the base of the scaffolds, pore size was relatively constant at 90 μm. The only exception was the scaffold with a set freezing temperature of -20 ºC, which had a significantly higher pore size of 115 μm. The lack of change to the pore size at the base of the scaffold with a thermal hold may be due to the relatively short time period of annealing, 3 hours, instead of the 18 hours determined in literature to produce a maximum increase in pore size [14].

4.4 Relationship Between Pore Structure and Thermal Parameters

Given the fundamental nature of ice templating, it was hypothesized that the thermal parameters relating to freezing could be used as a predictive measure of the final pore structure. It has already been observed that the nucleation temperature has a huge impact on scaffold structure, as it is chiefly responsible for whether scaffolds are isotropic or anisotropic [5, 7]. However, the present study found no correlation between nucleation temperature and the final pore size at the top of the scaffold. Within metallurgical literature, it has been found that very fine, equiaxed grain structures are not due purely to nucleation, but to a process termed “grain multiplication” which is dependent on dendrites remelting and remodeling during the solidification process [21]. Like metallurgical systems, primary nucleation events within ice are relatively rare, occurring infrequently and with considerable lag times between events [19]. In contrast, the growth rate of crystals is very fast, making it likely that the same principles in metallic alloys apply to collagen scaffold structures.

The scaffold structures obtained in this study were dependent on the efficiency of latent heat removal during crystallization, which was quantified by the parameter known as time at equilibrium. Indeed, a clear correlation existed between the time at equilibrium and pore size, which incorporated all experimental variables including changes to filling height, collagen weight percentage, and freezing protocol. The kinetics of crystal growth are known to be important to determining the size of features in anisotropic structures [22]. Here we demonstrate that not only the kinetics of ice crystal growth, but molecular diffusion during latent heat release is also critical. The relationship between time at equilibrium and pore size was dependent on $t^{1/n}$, with n = 4.8, which is different from the results reported for primary and secondary spacing of dendritic growth, where n = 2 or 3 [21]. The additional time dependence may reflect additional

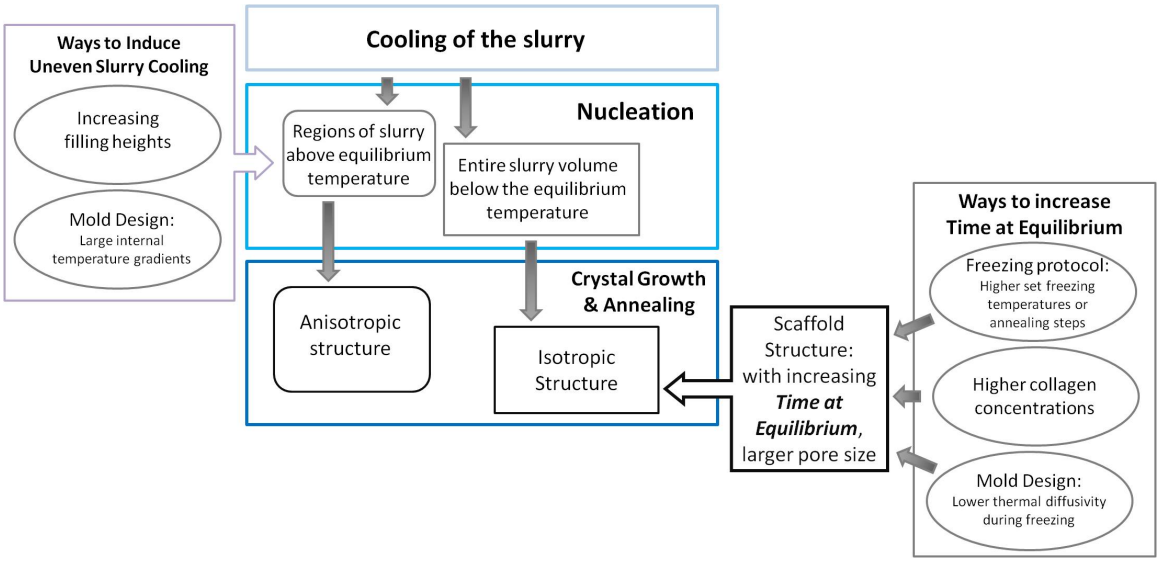

Figure 8: A flow chart summarizing the key points to creating scaffold structure and ways in which to alter the processing to tailor the scaffold structure.

processes which are important, and may be a result of nonlinear coupling between different energy scales, common to hydrodynamic systems [23, 24].

The dependence of scaffold structure on time at equilibrium highlights the fact that annealing plays a large role on the final scaffold structure, even before solidification has been completed. Thus, at the base of scaffolds, which quickly and consistently cooled below -1.5 ºC, the pore size remained constant at 90 μm, despite large changes in processing variables. However, at the top of the scaffolds, which had very different rates of latent heat conduction during freezing, the pore size was sensitive to processing parameters.

4.5 Toolkit for Tailoring Ice-Templated Scaffold Structure

Having demonstrated the fundamental link between the time at equilibrium and scaffold pore size, it is possible to summarize the effects of set processing variables on collagen scaffold structure. It has been shown previously that the nucleation step controls the anisotropy of the scaffold structure [7]. If a region of slurry has not yet reached the equilibrium freezing temperature when primary nucleation occurs, a condition which can be created through slurry filling height and mold design, an anisotropic scaffold results [16]. During the current study, it was found that variations in the freezing protocol, mold design and filling volume alter scaffold structure by changing the efficiency of latent heat removal from the solidifying slurry. In all cases, it was found that the universal principal to predict the final pore size was the amount of time which the slurry spent at equilibrium, regardless of the processing used to create that scaffold. All of the individual pieces together make a powerful toolkit for researchers to finely tune scaffold structure to their specific purpose, as illustrated in Figure 8.

The fact that this relationship is based on fundamental principles of ice templating, should

make this toolkit applicable to a wide variety of systems, such as pharmaceutical drugs and ceramic slurries. In addition, the scaffolds created during this study are large enough to span critical sized defects, being larger than 10 mm in all directions. We believe that with only a few number of experiments to map out the curve of pore size and time at equilibrium, these principles allow a curve to be constructed highlighting the necessary adjustments to customize the porous material.

5 Conclusions

In the current paper we have built a toolkit for tailoring the structure of isotropic collagen scaffolds. Altering both the set freezing temperature and adding a thermal hold in the freezing cycle had a significant effect on the freezing behavior of the slurry and the final pore size. It was found that within large isotropic scaffolds, greater than 10 mm in all dimensions, annealing occurs within the scaffold structure during the removal of latent heat. To measure the period of active crystal growth a thermal parameter called "time at equilibrium" was defined. The time at equilibrium had a direct correlation to pore structure, independent of the processing variables used to make the scaffolds: filling height, collagen concentration, mold design, and set freezing protocol. The robust, and fundamental, link between time at equilibrium and pore structure should be applicable to a wide range of ice-templating systems and allow researchers to easily customize porous materials.

References

[1] C. M. Murphy, M. G. Haugh, and F. J. O'Brien, "The effect of mean pore size on cell attachment, proliferation and migration in collagen-glycosaminoglycan scaffolds for bone tissue engineering," *Biomaterials* **31**(3), pp. 461–466, 2010.

[2] S. R. Caliari and B. A. C. Harley, "The effect of anisotropic collagen-gag scaffolds and growth factor supplementation on tendon cell recruitment, alignment, and metabolic activity," *Biomaterials* **32**(23), pp. 5330–5340, 2011.

[3] B. A. Harley, J. H. Leung, E. Silva, and L. J. Gibson, "Mechanical characterization of collagen-glycosaminoglycan scaffolds," *Acta Biomaterialia* **3**(4), pp. 463–474, 2007.

[4] A. Kureshi, U. Cheema, T. Alekseeva, A. Cambrey, and R. Brown, "Alignment hierarchies: engineering architecture from the nanometre to the micrometre scale," *Journal of the Royal Society Interface* **7**, pp. S707–S716, 2010.

[5] J. Searles, "Freezing and annealing phenomena in lyophilization," in *Freeze-Drying/Lyophilization of Pharmaceutical and Biological Products*, L. Rey and J. May, eds., ch. 4, Marcel Dekker, Inc., New York, 2nd ed., 2004.

[6] A. Hottot, S. Vessot, and J. Andrieu, "Freeze drying of pharmaceuticals in vials: Influence of freezing protocol and sample configuration on ice morphology and freeze-dried cake texture," *Chemical Engineering and Processing* **46**(7), pp. 666–674, 2007.

[7] K. M. Pawelec, A. Husmann, S. M. Best, and R. E. Cameron, "Understanding anisotropy and architecture in ice-templated biopolymer scaffolds." Manuscript submitted.

[8] N. Y. Yuan, Y. A. Lin, M. H. Ho, D. M. Wang, J. Y. Lai, and H. J. Hsieh, "Effects of the cooling mode on the structure and strength of porous scaffolds made of chitosan, alginate, and carboxymethyl cellulose by the freeze-gelation method," *Carbohydrate Polymers* **78**(2), pp. 349–356, 2009.

[9] F. J. O'Brien, B. A. Harley, I. V. Yannas, and L. Gibson, "Influence of freezing rate on pore structure in freeze-dried collagen-gag scaffolds," *Biomaterials* **25**(6), pp. 1077–1086, 2004.

[10] C. S. Lindenmeyer, G. T. Orrok, K. A. Jackson, and B. Chalmers, "Rate of growth of ice crystals in supercooled water," *Journal of Chemical Physics* **27**(3), pp. 822–822, 1957.

[11] F. J. O'Brien, B. A. Harley, I. V. Yannas, and L. J. Gibson, "The effect of pore size on cell adhesion in collagen-gag scaffolds," *Biomaterials* **26**(4), pp. 433–441, 2005.

[12] S. Deville, J. Adrien, E. Maire, M. Scheel, and M. Di Michiel, "Time-lapse, three-dimensional in situ imaging of ice crystal growth in a colloidal silica suspension," *Acta Materialia* **61**(6), pp. 2077–2086, 2013.

[13] A. Myerson and R. Ginde, "Crystals, crystal growth and nucleation," in *Handbook of Industrial Crystallization*, A. Myerson, ed., ch. 2, pp. 33–62, Butterworth-Heinemann, 2nd ed., 2002.

[14] M. G. Haugh, C. M. Murphy, and F. J. O'Brien, "Novel freeze-drying methods to produce a range of collagen-glycosaminoglycan scaffolds with tailored mean pore sizes," *Tissue Engineering Part C-Methods* **16**(5), pp. 887–894, 2010.

[15] M. E. Kolewe, H. Park, C. Gray, X. Ye, R. Langer, and L. E. Freed, "3d structural patterns in scalable, elastomeric scaffolds guide engineered tissue architecture," *Advanced Materials* **doi: 10.1002/adma.201301016**, 2013.

[16] K. M. Pawelec, A. Husmann, S. M. Best, and R. E. Cameron, "The influence of mold design on freeze-dried scaffold structure homogeneity." Manuscript submitted.

[17] C. Wilson, "Texture and grain growth during the annealing of ice," *Textures and Microstructures* **5**, pp. 19 – 31, 1982.

[18] A. M. Padilla, S. G. Chou, S. Luthra, and M. J. Pikal, "The study of amorphous phase separation in a model polymer phase-separating system using raman microscopy and a low-temperature stage: Effect of cooling rate and nucleation temperature," *Journal of Pharmaceutical Sciences* **100**(4), pp. 1362–1376, 2011.

[19] A. F. Heneghan, P. W. Wilson, G. M. Wang, and A. D. J. Haymet, "Liquid-to-crystal nucleation: Automated lag-time apparatus to study supercooled liquids," *Journal of Chemical Physics* **115**(16), pp. 7599–7608, 2001.

[20] J. A. Searles, J. F. Carpenter, and T. W. Randolph, "The ice nucleation temperature determines the primary drying rate of lyophilization for samples frozen on a temperature-controlled shelf," *Journal of Pharmaceutical Sciences* **90**(7), pp. 860–871, 2001.

[21] M. C. Flemings, *Solidification Processing*, Materials Science and Engineering, McGraw-Hill Book Co, New York, 1974.

[22] S. Deville, "Freeze-casting of porous ceramics: A review of current achievements and issues," *Advanced Engineering Materials* **10**(3), pp. 155–169, 2008.

[23] M. Kawaji, "Macroscopic and microscale phenomena in multiphase energy storage and transport systems," *Journal of Heat Transfer-Transactions of the Asme* **134**(3), 2012. Times Cited: 0 0.

[24] D. J. Tritton, *Physical Fluid Dynamics*, Van Nostrand Reinhold, New York, 1977.